Supplementary Figures

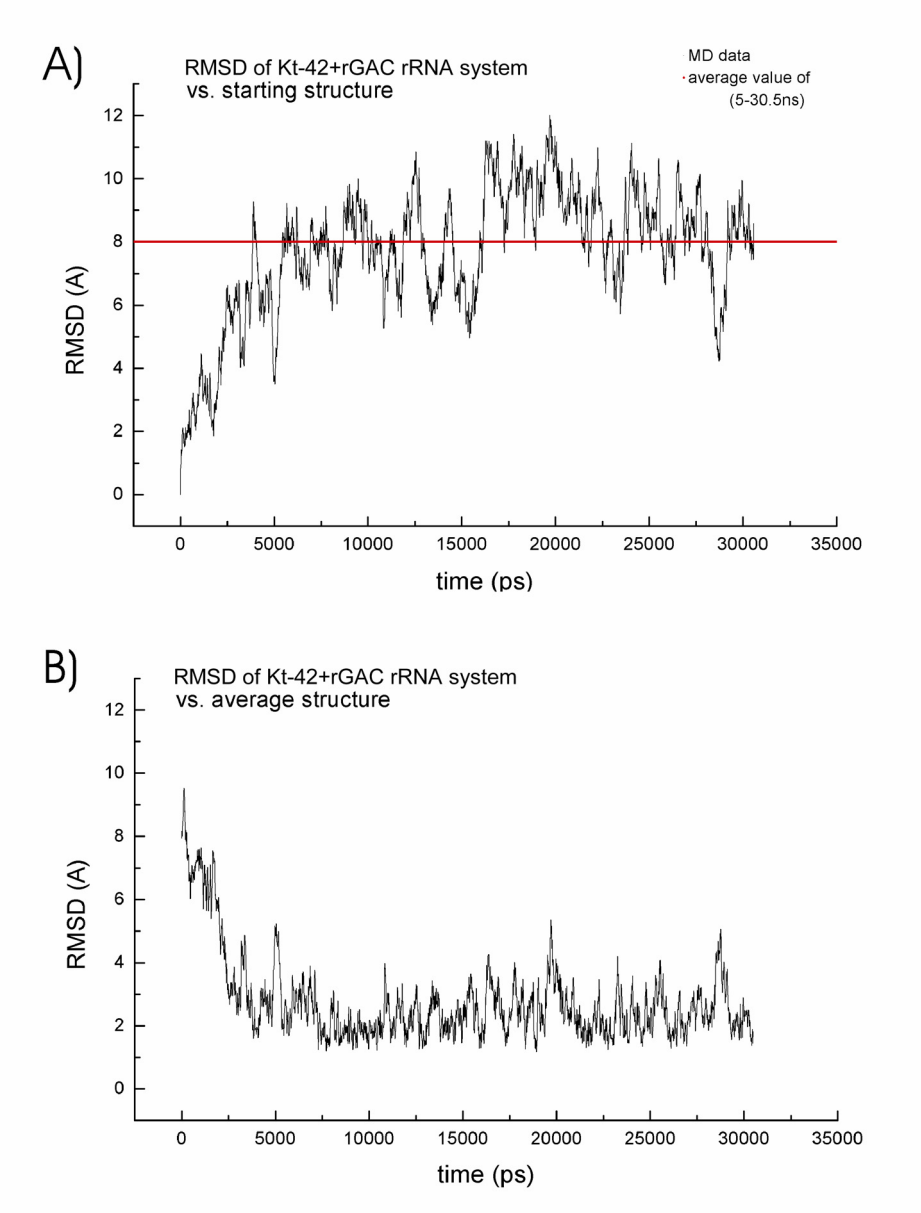

Figure S1. RMSd of coordinate positions of the Kt-42+rGAC system. A) RMSd vs. starting structure. The red line represents the average RMSd value after the initial relaxation (0-5ns). The system then fluctuates. B) RMSd vs. average structure over 5000-30500 ps time interval.

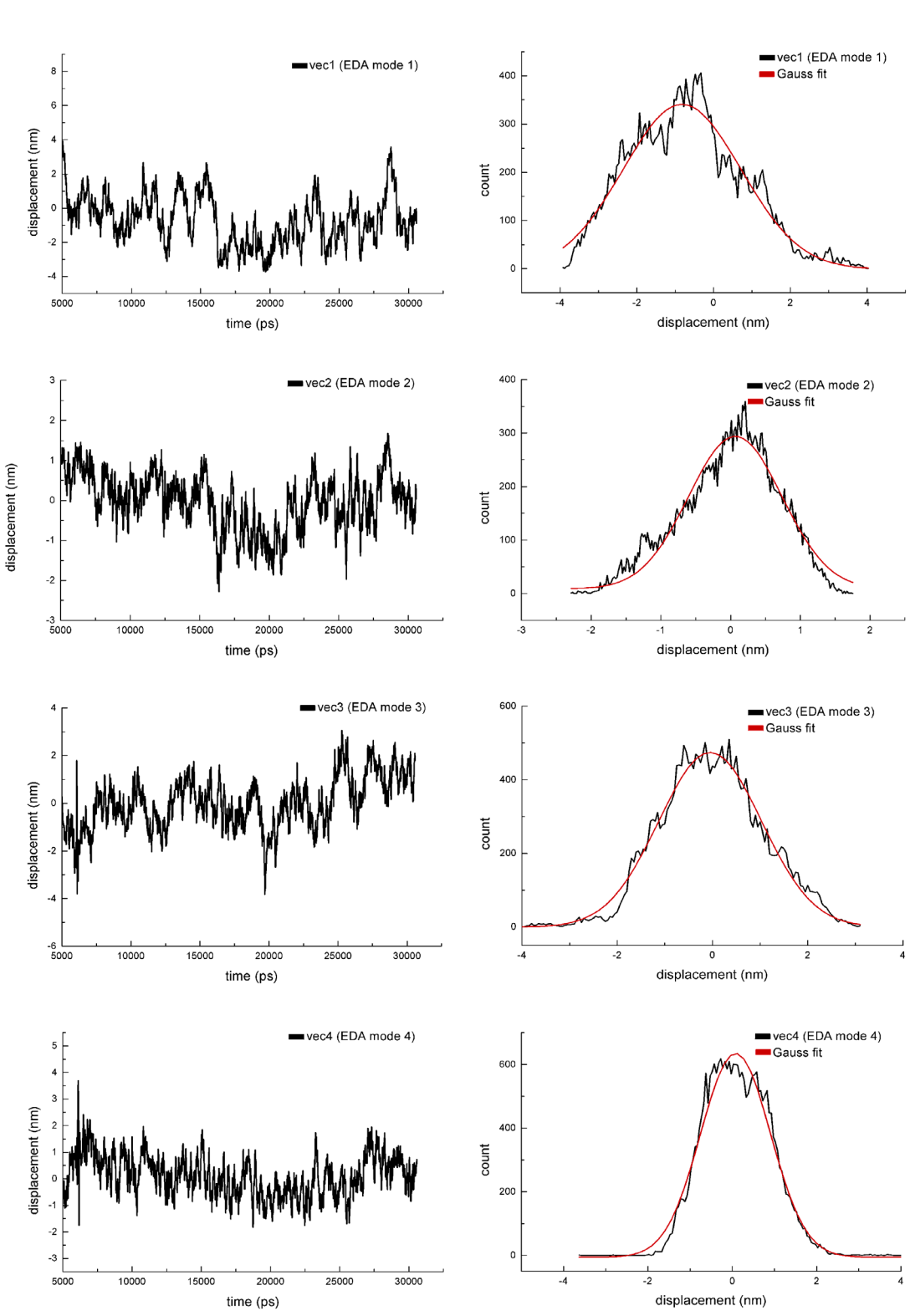

Figure S2. Displacements along EDA modes 1-4. Motions along eigenvectors 1-4 from P coordinates covariance matrix (left) and their displacement distributions (right). Red line represents Gaussian fit. The first 5 ns were not considered for EDA analysis (see the text).

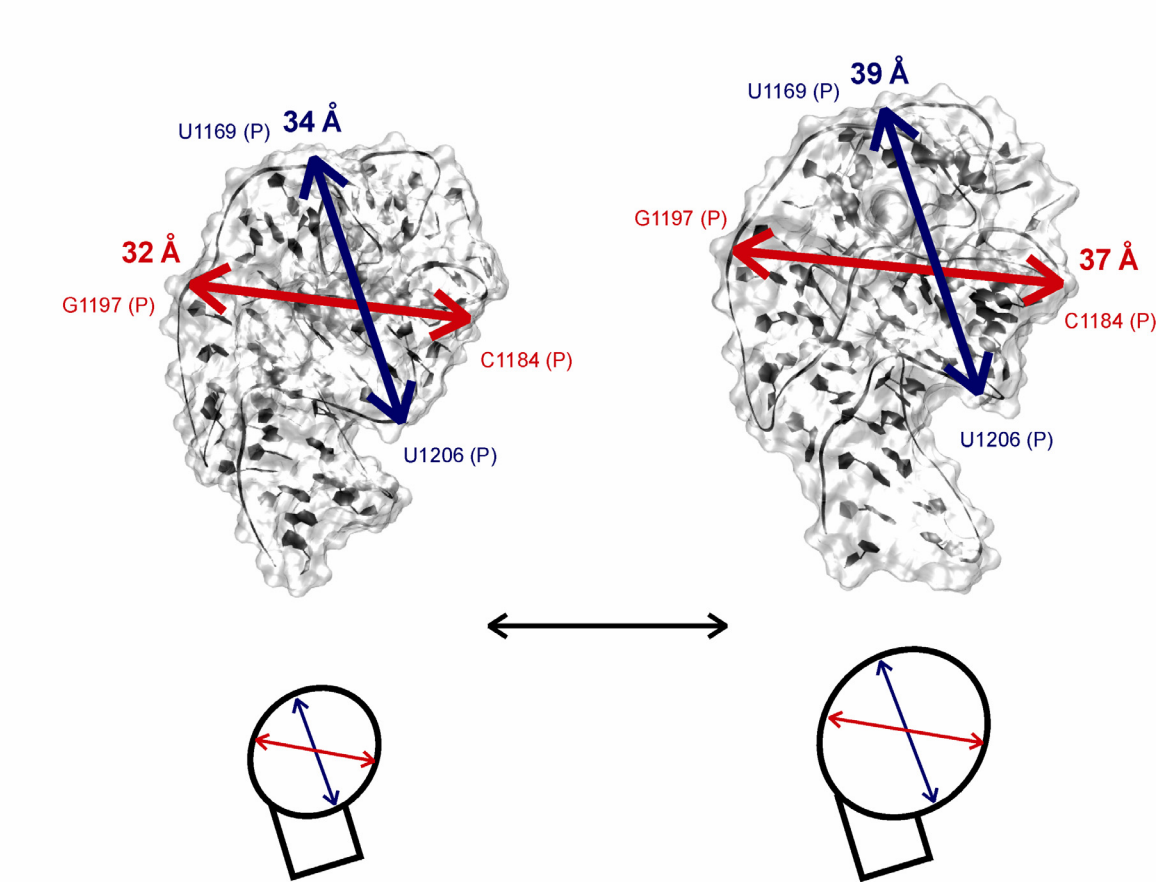

Figure S3. Internal breathing of rGAC (EDA mode 2) not associated with displacement of distant parts of the simulated Kt-42+rGAC system. Top) reversible inflation (snapshots with maximal observed deviation) of the rGAC within the range of ca. 5 Å measured as G1197(P)-C1184(P) and U1169(P)-U1206(P) distances. Bottom) schematic representation.

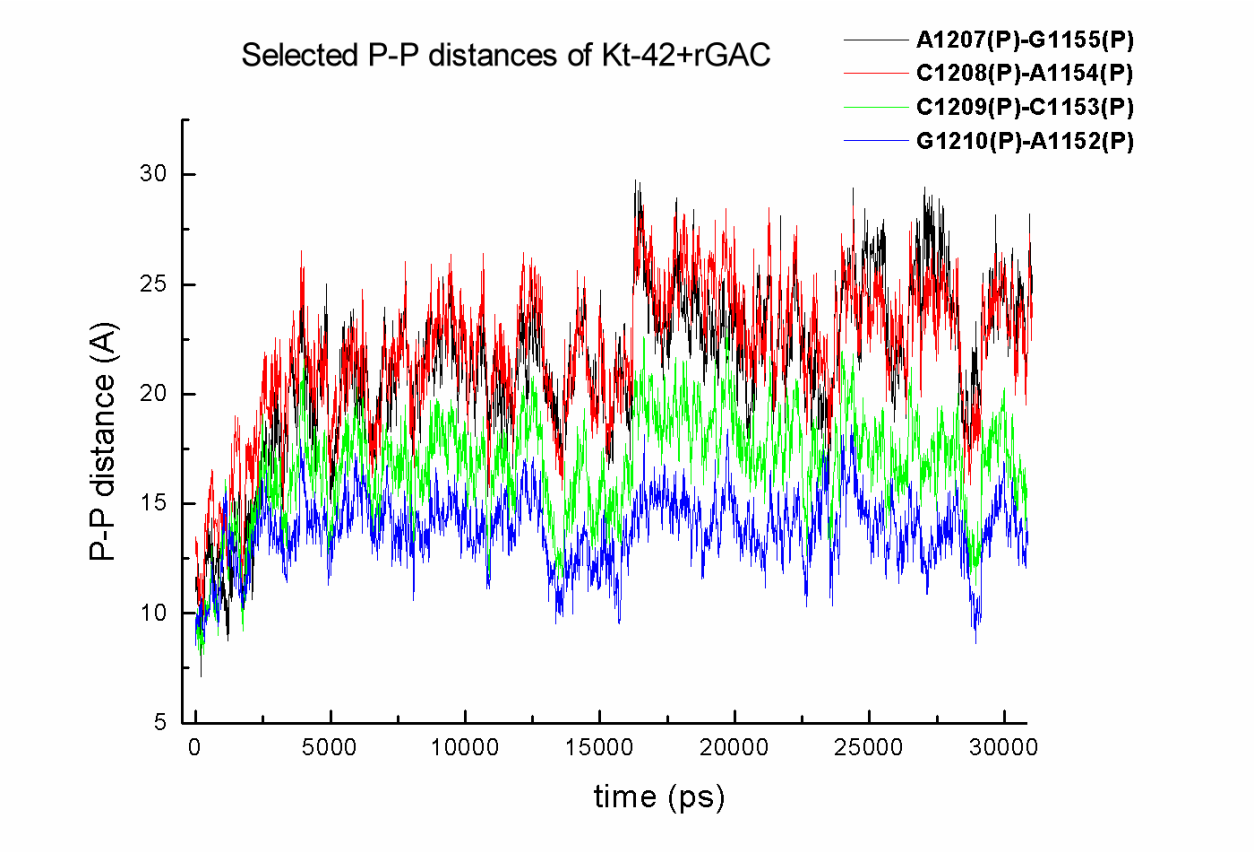

Figure S4. Time traces of selected inter-phosphate distances indicating the initial (0-5ns) return from bent (x-ray) geometry of the duplex composed of the upper part of Helix 42 and Helix 43 to straight, canonical-like RNA geometry.

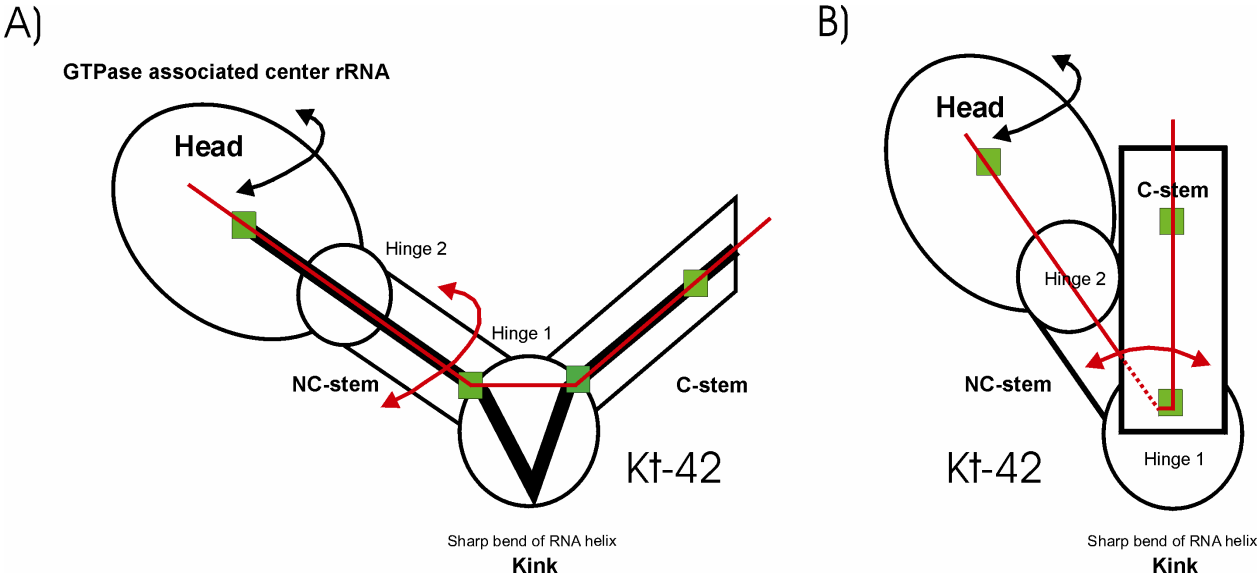

Figure S5. Twisting of Kt-42+rGAC system.
A) Scheme indicating the centers of mass (green) used for calculation of the fictive dihedral angle (Figure S6, see Materials and methods). Black arrow indicates the reversible twisting of the *Head* around the *NC-stem* of Kt-42 while red arrow indicates the twisting propagating from the Kt-42's internal loop resulting in coupled complex twisting motion of the Kt-42+rGAC system. B) Orthogonal view.

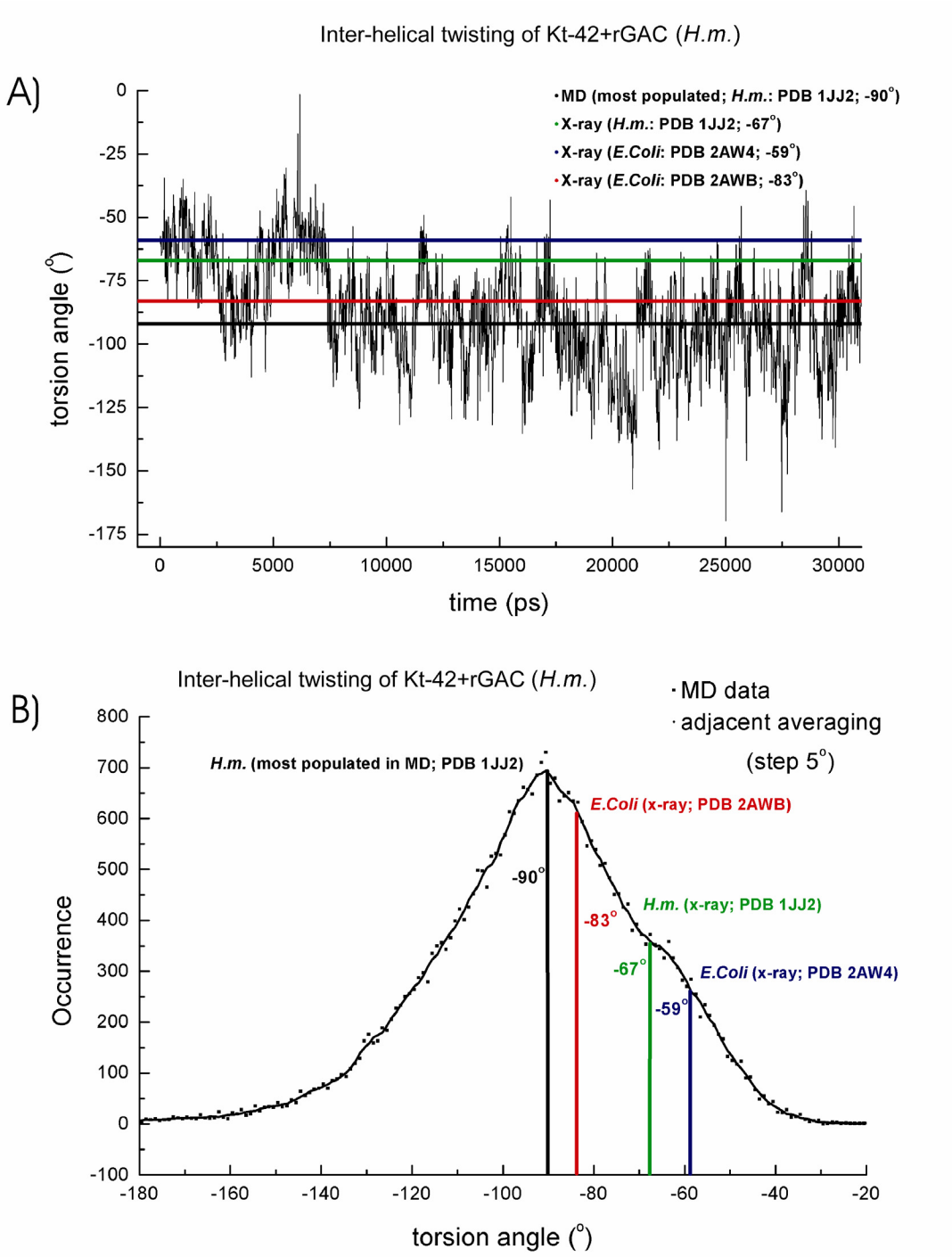

Figure S6. Kt-42+rGAC twisting flexibility.
A) Time trace of the fictive dihedral angle (see Material and methods) of Kt-42+rGAC rRNA system. Color codes show comparison of MD with available crystal structures of *H.m.* (1JJ2) and *E.coli* (2AW4 and 2AWB). B) Histogram indicates occurrence of two slightly preferred values of fictive dihedral angle sampled during MD. The overall broad distribution indicates that these preferred positions are probably close in free energy and are easily accessible, so that we deal with a broad range of low energy structures. X-ray values are marked by color codes.

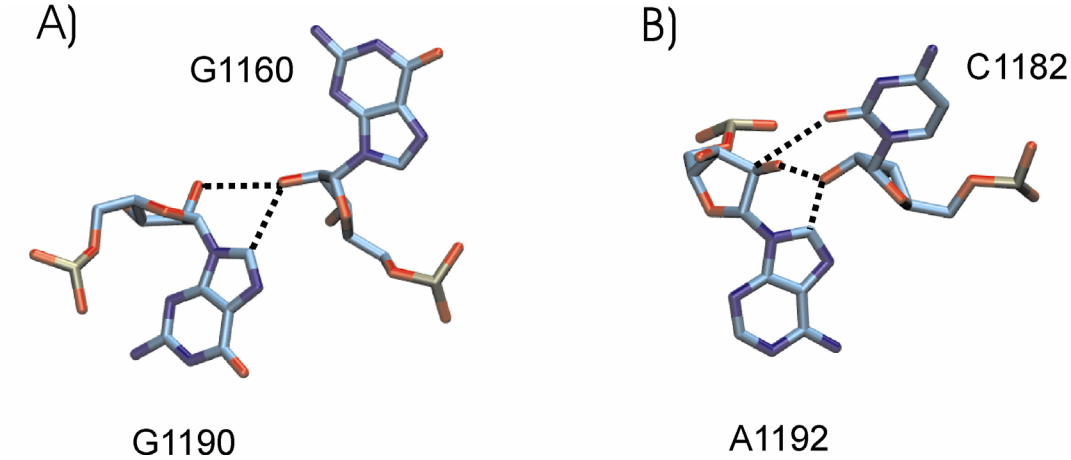

Figure S7. Bifurcated interaction – a possible new type of base pairing. A) Bifurcated H-bonds between O2' of G1160 and O2' and C8 of G1190. B) Bifurcated H-bonds between O2‘ of C1182 and O2‘ and C8 of A1192, and contact between C1182(O2) and A1192(C2'). Both interactions are taken from the x-ray structure of *H.m.* with PDB code 1JJ2.

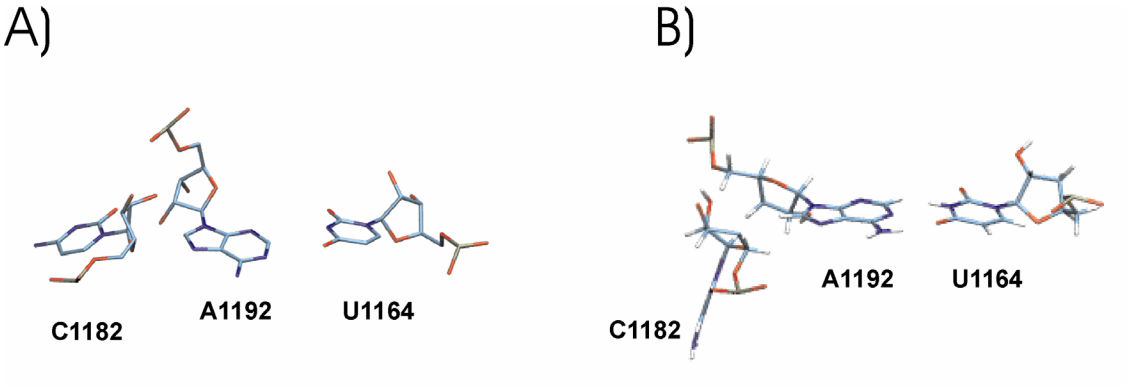

Figure S8. Coplanar vs. perpendicular arrangement of U1164-A1192/C1182 base triad. A) the X-ray arrangement of U1164-A1192/C1182 triad from *H.m.* crystal structure (PDB code 1S72) with C1182 coplanar with the A-U base pair and forming *trans* SE/SE A1192/C1182 interaction. B) MD arrangement (formed during early stages of equilibration and stable during simulation) with C1182 perpendicular to A-U base pair. This arrangement reveals gentle dynamical behavior during MD without breaking of perpendicularity (see Figure S12F).

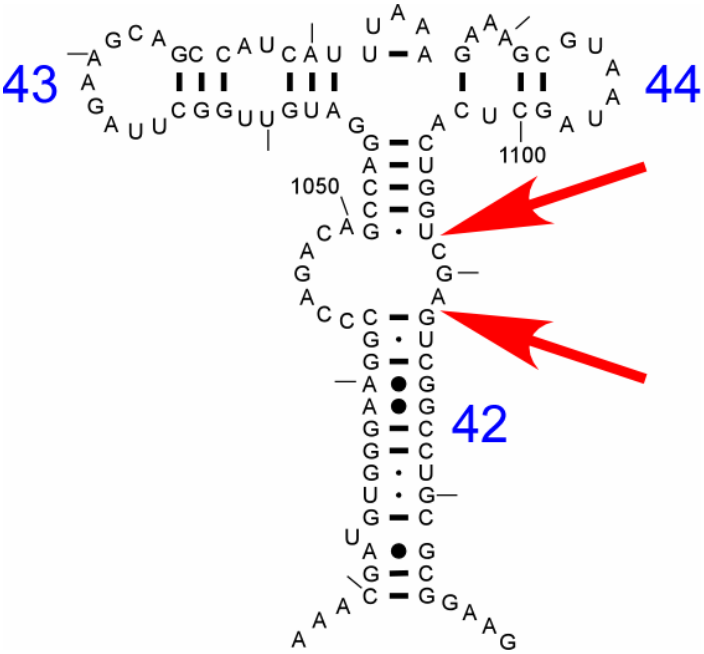

Figure S9. Location of the insertions in about 15% of bacterial sequences (red arrows). The graph represents the secondary structure of *E.coli* (1).

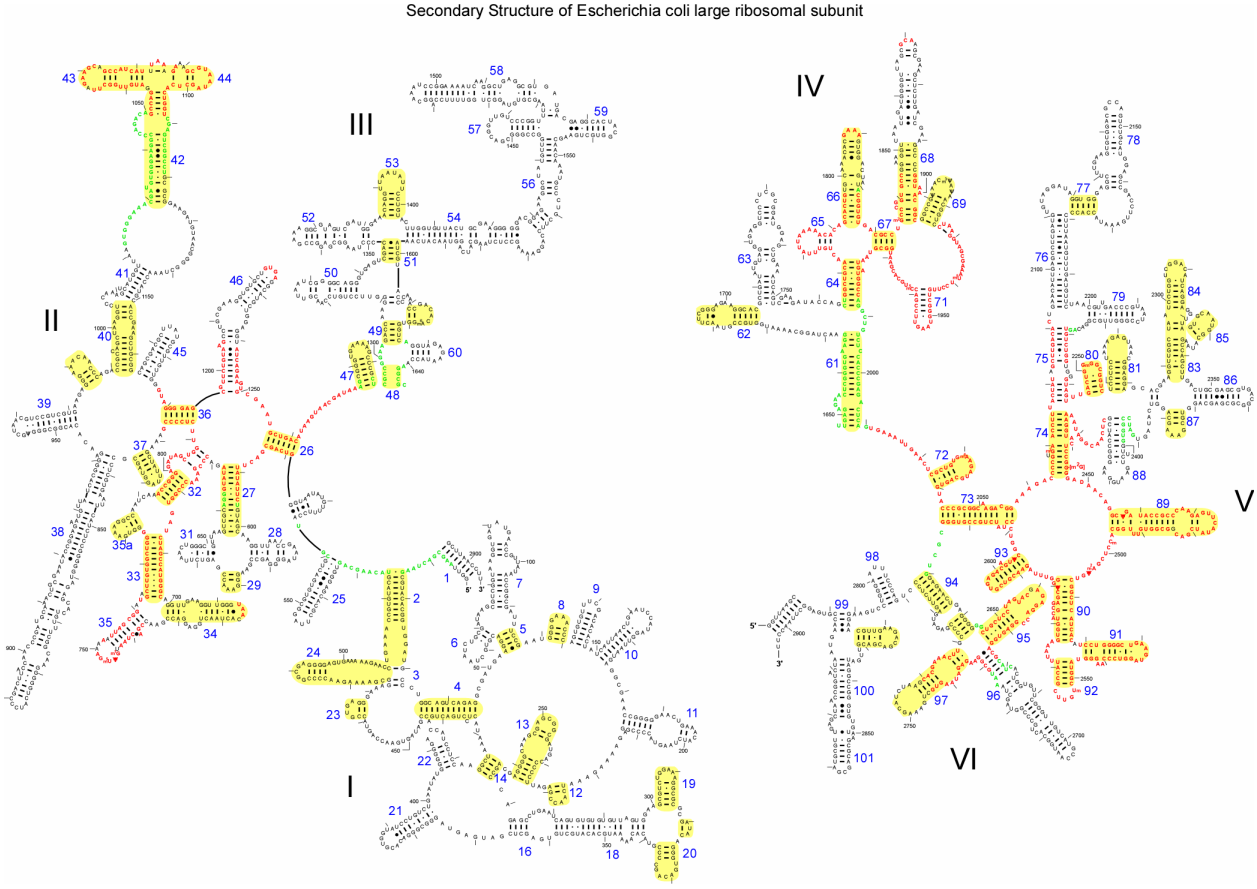

Figure S10. Conservation of helix lengths in the large ribosomal subunit. Helices shaded in yellow are conserved in length among all three domains of life (ca. 58 conserved helices out of 115). Red nucleotides are present in all three domains and in the two organelles, and can be structurally aligned with the *H.marismortui* ribosomal subunit. Green nucleotides are present in the three domains and the two organelles but can not be easily aligned. The graph represents *E.coli* secondary structure based on (1). Nucleotide colors are based on (2).

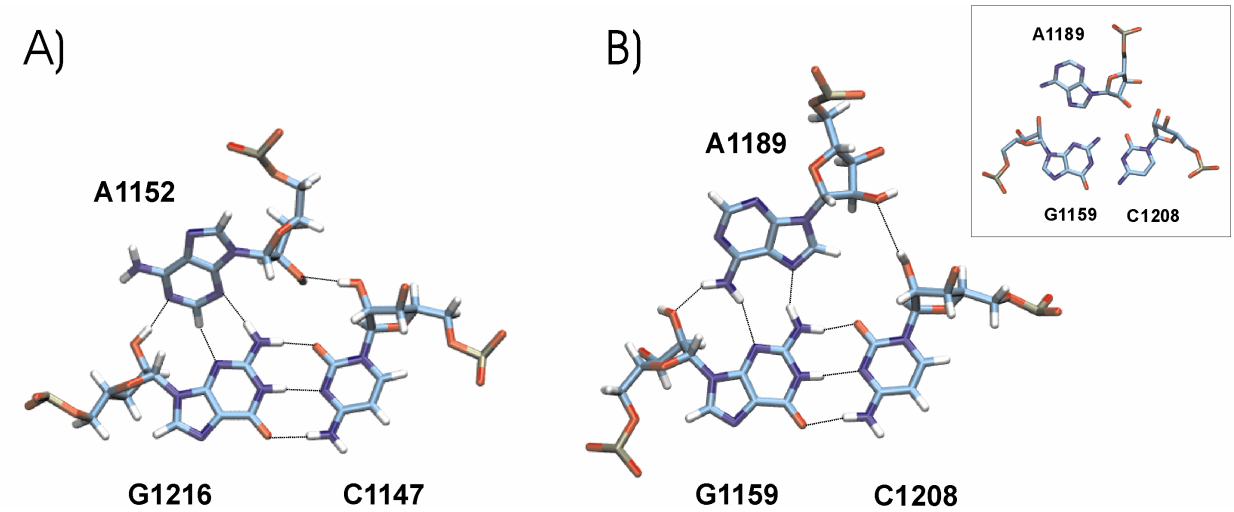

Figure S11. A-minor type I vs. *trans* H/SE interaction.
A) A-minor type I interaction, reported by Nissen et al.(3) from Kt-42 (*Hinge1*) B) *trans* H/SE A/G interaction of A1189/G1159=C1208 triad, localized at the border between Helix 42 and rGAC (*Hinge2*). These bases form A-minor type I interaction in the available *D.r.* (1NKW) and *E.coli* (2AW4 and 2AWB) ribosomal structures. The inset indicates the actual x-ray (starting) position of bases with A1189 modestly shifted away from the G1159. The position of A1189 changes during the first stages of equilibration and forms *trans* H/SE interaction that remains stable. Both triads (A-minor type I and the triad containing *trans* H/SE) reveal dynamical behavior, directly coupled with presence (*open*) or absence (*closed*) of water molecule between the interacting C/A (see text and Razga et al.(4)).

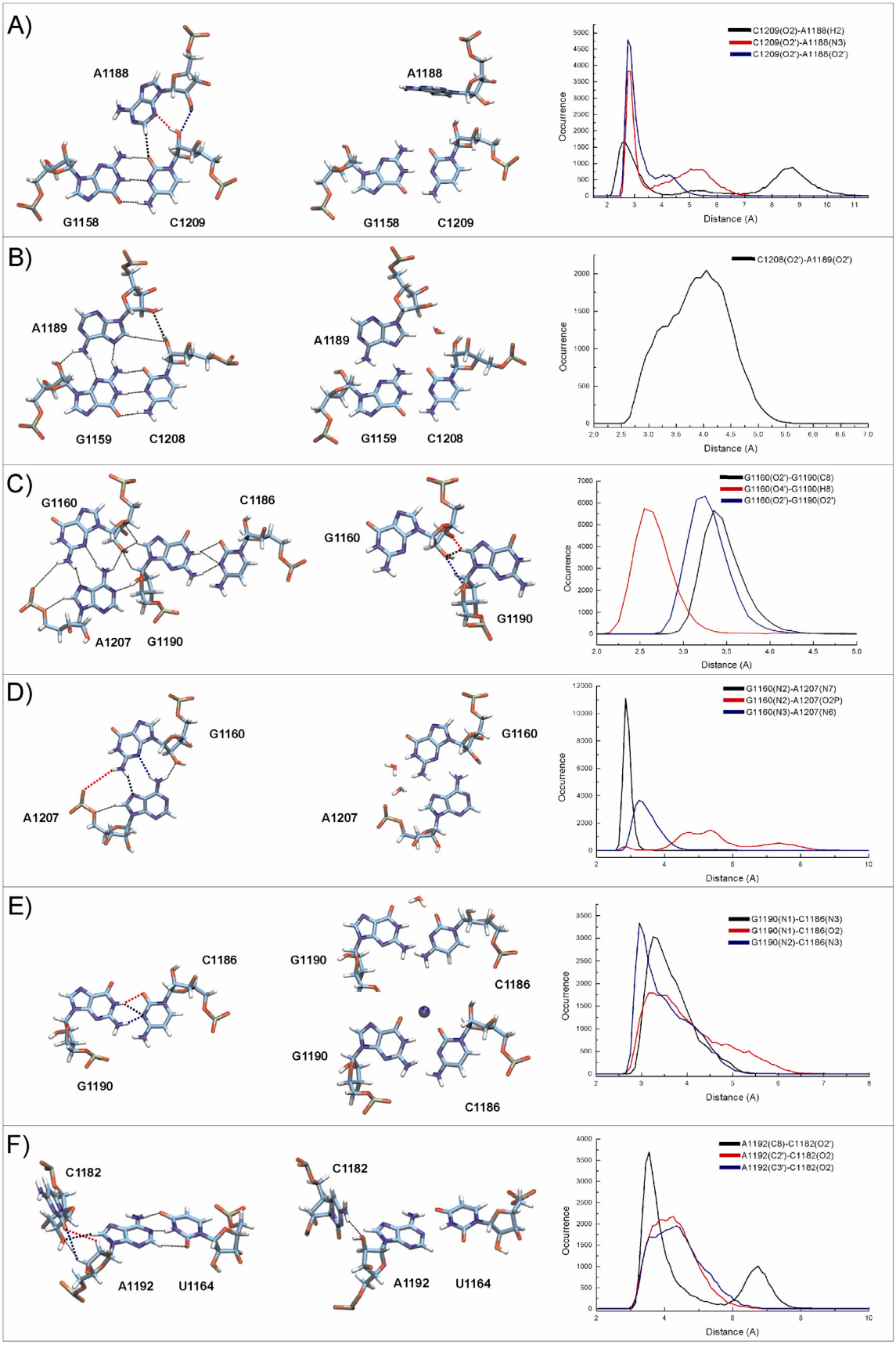
A)
A1188
G1158
C1209
A1188
G1158
C1209
C1209(O2)-A1188(H2)
C1209(O2')-A1188(N3)
C1209(O2')-A1188(O2')
Occurrence
Distance (A)
B)
A1189
G1159
C1208
A1189
G1159
C1208
C1208(O2')-A1189(O2')
Occurrence
Distance (A)
C)
G1160
C1186
A1207
G1190
G1160
G1190
G1160(O2')-G1190(C8)
G1160(O4')-G1190(H8)
G1160(O2')-G1190(O2')
Occurrence
Distance (A)
D)
G1160
A1207
G1160
A1207
G1160(N2)-A1207(N7)
G1160(N2)-A1207(O2P)
G1160(N3)-A1207(N6)
Occurrence
Distance (A)
E)
C1186
G1190
G1190
C1186
G1190
C1186
G1190(N1)-C1186(N3)
G1190(N1)-C1186(O2)
G1190(N2)-C1186(N3)
Occurrence
Distance (A)
F)
C1182
A1192
U1164
C1182
A1192
U1164
A1192(C8)-C1182(O2')
A1192(C2')-C1182(O2)
A1192(C3')-C1182(O2)
Occurrence
Distance (A)

Figure S12. Structure and dynamics of base pairs contributing to the internal breathing of rGAC (*Hinge2* and Helix 43). Representative MD substates (left and middle) and histogram profiles (right) of selected distances.

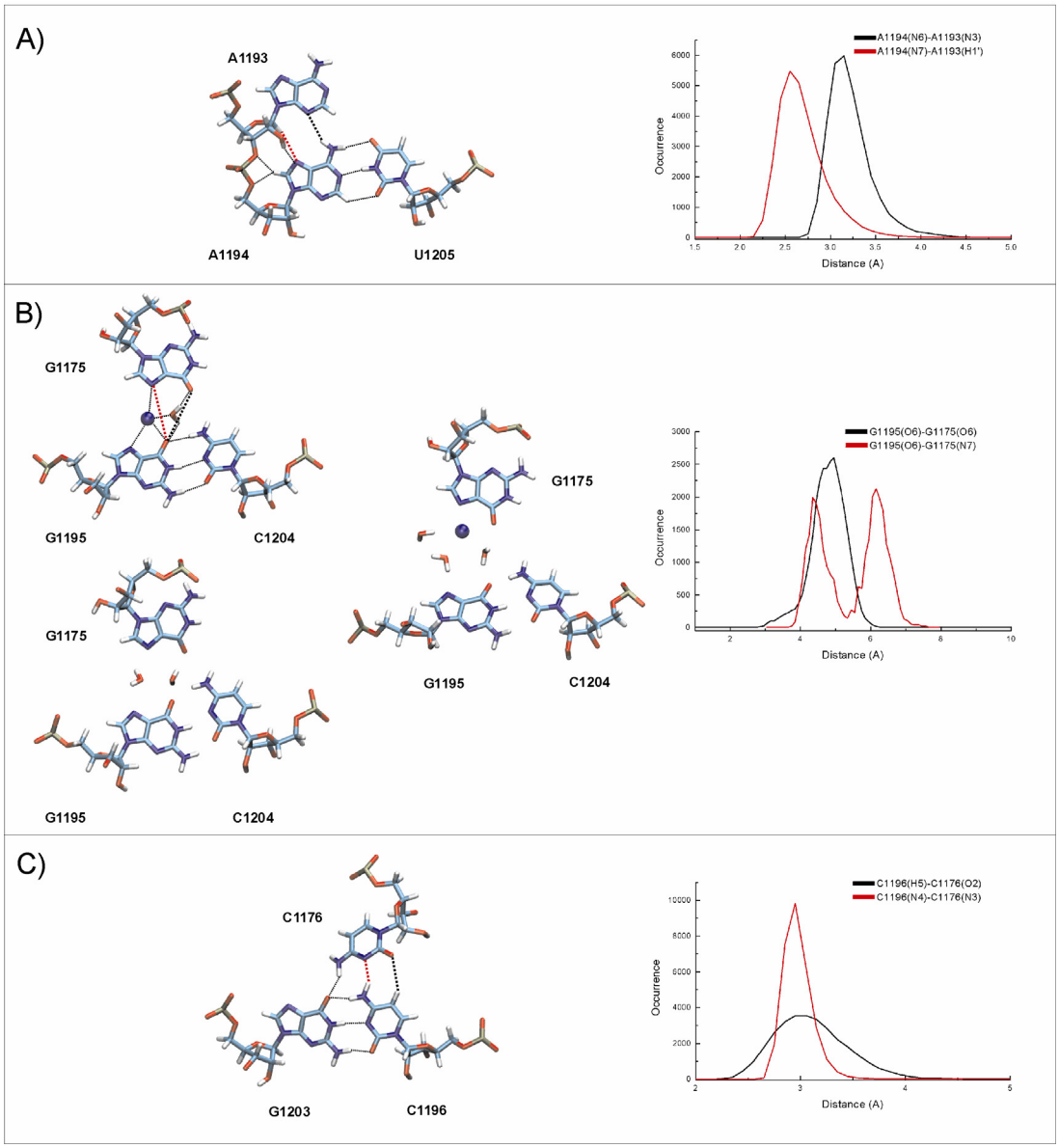

Figure S13. Dynamics of base pairs contributing to the internal breathing of rGAC (Helix 44). Individual conformations (left) and histogram profiles (right) of selected distances.

1. Cannone, J.J., Subramanian, S., Schnare, M.N., Collet, J.R., D'Souza, L.M., Du, Y.S., Feng, B., Liu, N., Madabushi, L.V., Muller, K.M. et al. (2002) The comparative RNA web (CRW) site: an online database of comparative sequence and structure information for ribosomal, intron, and others RNAs. BMC Bioinformatics, **3**, 2.
2. Mears, J.A., Cannone, J.J., Stagg, S.M., Gutell, R.R., Agrawal, R.K. and Harvey, S.C. (2002) Modeling a minimal ribosome based on comparative sequence analysis. J. Mol. Biol., **321**, 215-234.
3. Nissen, P., Ippolito, J.A., Ban, N., Moore, P.B. and Steitz, T.A. (2001) RNA tertiary interactions in the large ribosomal subunit: The A-minor motif. Proc. Natl. Acad. Sci. USA, **98**, 4899-4903.

4. Razga, F., Koca, J., Sponer, J. and Leontis, N.B. (2005) Hinge-like motions in RNA Kink-turns: The role of the second A-minor motif and nominally unpaired bases. Biophys. J., **88**, 3466-3485.